Effects of local fields in time-dependent density functional theory shown in oxidized silicon clusters

Matteo Gatti and Giovanni Onida
Istituto Nazionale per la Fisica della Materia and Dipartimento di Fisica dell'Università di Milano, via Celoria 16, I-20133 Milano, Italy

(Received 14 December 2004; revised manuscript received 28 February 2005; published 21 July 2005)

We studied the influence of oxygen and oxygen-related bonds on the structural, electronic, and optical properties of a prototypical silicon dot, the adamantanelike $Si_{10}H_{16}$ nanocrystal. The optical photoabsorption spectra have been calculated keeping into account both local field effects and the effects of pseudopotential nonlocality. While the effects of the latter show up essentially as a change of a few percent of the *f*-sum rule integral, the former are shown to modify substantially both the optical absorption edge and the size of its redshift as induced by oxidation of the nanocrystal. Exchange-correlation contributions have also been evaluated, within the adiabatic local density approximation.

DOI: 10.1103/PhysRevB.72.045442 PACS number(s): 73.22.−f, 78.67.Bf, 71.15.Qe

I. INTRODUCTION

In the last years the interest in the electronic and optical properties of silicon nanocrystals has been continuously increasing. On one hand, the way towards the achievement of efficient visible light emission from silicon has been opened since the discovery of photoluminescence from porous silicon[1] and, more recently, of optical gain in silicon nanocrystals embedded in a SiO_2 matrix.[2] On the other hand, silicon clusters are also ideal models to study the effects related to the reduction in size of semiconductors. In these systems, both quantum confinement effects (opening of quasiparticle gap, enhancement of excitonic effects), and surface effects (passivation, reconstruction, defects) play a fundamental role.

There exist many different calculations of the energy gap of silicon nanocrystals as a function of their size. However, significant differences are often found between theoretical predictions[3] and experimental measurements.[4] In particular, the observed *optical gap* is generally smaller than the calculated one. Moreover, these systems display large Stokes shifts (i.e., difference between absorption and emission energies),[5,6] which must be taken into account when photoluminescence (PL) experiments are compared to calculations of the optical gap. Another source of difficulty comes from the fact that experiments are sometimes lacking a precise control of the cluster size, and even of their chemical composition. It is still more difficult to access experimentally the structural details of the nanocrystal, while reconstruction effects (similar to those encountered in surfaces[7]) can be very important in the determination of the optical properties. On the theoretical side, the many available calculations are often effectuated within very different degrees of approximation, and different levels of accuracy, even the definition of "gap" is not always unanimous. For example, calculations for large clusters (thousands of atoms) have been performed by semiempirical models,[8] relying on the transferability of parameters from the bulk. However, semiempirical models may be too rough for the study of deeply reconstructed systems, as shown, e.g., in Fig. 4 of Ref. 9. *Ab initio* calculations, based, e.g., on density functional theory (DFT), can be more reliable, but are limited to small nanocrystals (about 10^2 atoms) due to the large computational weight.

In recent experiments on silicon dots in porous silicon[10] a redshift of PL, immediately after the exposure of the Si dots to air, has been observed. These findings have been confirmed by the calculations of Puzder *et al.*[11] and Luppi and Ossicini.[12] Both works show that the formation of a double bond between silicon and oxygen strongly reduces the optical gap of small silicon nanocrystals, while single bond passivants have a less remarkable effect. In addition, the strongest redshift is obtained with the formation of the first double bond,[12] and a sort of saturation with increasing oxidation is observed.

The aim of the present work is twofold, on the one hand, we wish to clarify the role played by different theoretical approximations that can be adopted within the *ab initio* DFT-based scheme, obtaining also a quantitative estimate of the error bars due to numerical convergence; on the other hand, we investigate the mechanisms involved in the modification of the electronic and optical properties of Si nanocrystals when they are oxidized.

We have studied eight different clusters. SiH_4 (silane) and H_2SiO (silanone) are the simplest systems considered (top row of Fig. 1). Reliable experimental data (e.g., Ref. 26) to compare with our results exist for them, therefore, they have been taken as test cases. We have simulated the oxidation considering the adamantanelike $Si_{10}H_{16}$ nanocrystal (left of the second row in Fig. 1), and by adding an oxygen atom to its ground state structure. This can be made either without removing H atoms (hence leading to $Si_{10}H_{16}O$, shown on the right of the second row of Fig. 1, with an O atom placed on one of the 12 equivalent Si-Si bonds of $Si_{10}H_{16}$), or by replacing a pair of hydrogens with one oxygen (in this case, no Si-Si bond is broken). In the latter case, one is lead to one of the four different isomers of $Si_{10}H_{14}O$, shown on the two bottom rows of Fig. 1. In all the isomers, oxygen is covalently bonded to silicon, with either a double bond ("double" isomer, left of the third row, containing a Si=O bond like in the silanone H_2SiO structure), or with different

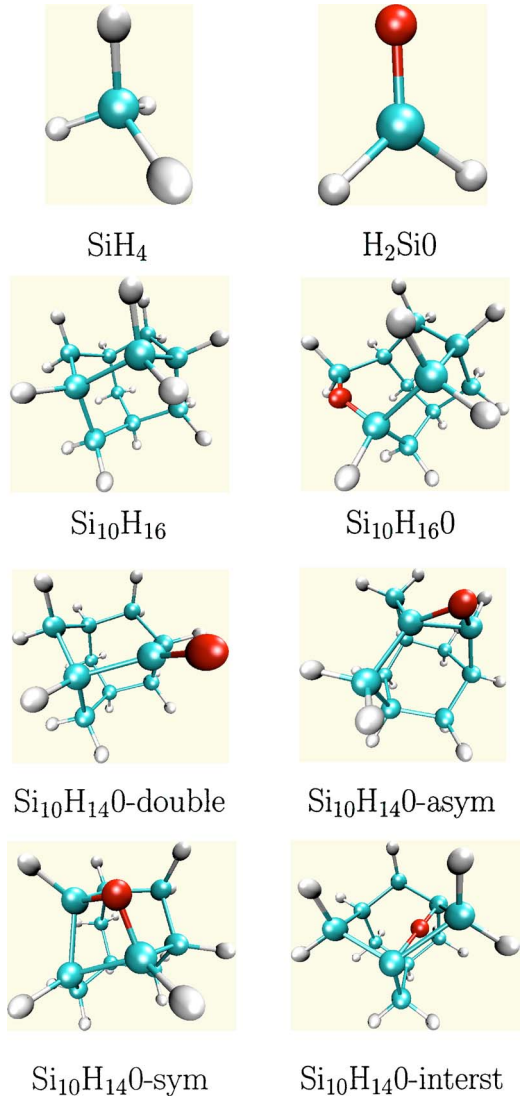

FIG. 1. (Color online) Structure of SiH_4, H_2SiO, $Si_{10}H_{16}$, $Si_{10}H_{16}O$ and the four isomers of $Si_{10}H_{14}O$. In the ball and stick representation, Si is light blue (gray), H is gray (light gray), and O is red (dark gray). In the case of silanone, the simplest Si_nH_mO system, the HOMO and LUMO Kohn-Sham orbitals are both oxygen-related p-like orbitals, with the HOMO lying in the plane containing the two H atoms, and the LUMO lying in the orthogonal plane.

kinds of bridge (i.e., Si-O-Si) bonds. In particular, oxygen can make a bridge between two "first neighbors" or "second neighbors" Si atoms ("asym" and "sym" isomers, shown, respectively, on the right of the third row and on the left of the bottom row), or it can lay in an "interstitial" position inside the Si_{10} cage ("interst" isomer, bottom-right of the figure).

The paper is organized as follows: first, we give a brief summary of the theory employed to compute the optical spectra with inclusion of local field and exchange-correlation effects, with some emphasis on the differences between the case of a finite cluster and that of an infinite (bulk) system. Then, in Sec. III, we first illustrate our results for the ground state properties (equilibrium geometries) and the Kohn-Sham electronic structure, studying in detail the effects of oxidation. In the following, we consider the optical spectra, calculated for SiH_4, H_2SiO, and for the different isomers of $Si_{10}H_{14}O$. We compare our results with experimental data (where available) and with several existing calculations, and we draw our conclusions in Sec. IV. Finally in the appendix we analyze the degree of numerical convergence which can be reached for the considered systems.

II. THEORY

The first ingredient for computing the optical properties is a reliable calculation of the ground state geometry. In the case of small clusters, the Car-Parrinello method[13] is an efficient and reliable tool allowing one to search for the equilibrium structure, by a simultaneous minimization of the energy with respect to the ionic and electronic degrees of freedom within density functional theory. Moreover, Kohn-Sham orbitals and eigenvalues, which are a byproduct of the total energy calculation, can be used as a starting point for excited-state calculations, either in many-body perturbation theory [GW plus Bethe-Salpeter equation (BSE)] or in a time-dependent density functional theory (TDDFT) scheme (for a recent review, see Ref. 14). Both these approaches make possible going beyond the so-called "single-quasiparticle approximation," by including, e.g., excitonic effects and/or local field effects. Many-body perturbation theory is physically more transparent, but can be numerically cumbersome, whereas TDDFT is numerically more efficient, but is still missing an efficient approximation for the exchange-correlation kernel. However, even the simple time-dependent local density approximation (TDLDA) is known to yield good results for finite systems, where the local field effects are predominant.[14]

In bulk systems the absorption spectrum is given by the imaginary part of the macroscopic dielectric function ε_M, which can be calculated in function of the energy ω as

$$\varepsilon_2(\omega) \equiv \mathrm{Im}\{\varepsilon_M(\omega)\} = -\lim_{\mathbf{q}\to 0} \mathrm{Im}\{v_{G=0}(\mathbf{q})\bar{\chi}_{G=G'=0}(\mathbf{q},\omega)\}. \tag{1}$$

Here G and G' are reciprocal lattice vectors, the limit for small momentum $\mathbf{q}$ corresponds to the dipole approximation, and $\bar{\chi}$ is a modified response function, related to the independent particle polarizability χ^0 by

$$\bar{\chi}_{G,G'} = \chi^0_{G,G'} + \sum_{G_1,G_2} \chi^0_{G,G_1}(\bar{v}_{G_1}\delta_{G_1,G_2} + f^{xc}_{G_1,G_2})\bar{\chi}_{G_2,G'} \tag{2}$$

f_{xc} is the exchange-correlation kernel and $\bar{v}_G$ is the Coulomb interaction without the long-range ($v_{G=0}$) term (see Ref. 14). The independent particle polarizability, $\chi^0_{G,G'}$, is given by the Fourier transform of

$$\chi^0(r,r',\omega) = 2\sum_{ij} f_i(1-f_j)\psi_i^*(r)\psi_j(r)\psi_j^*(r')\psi_i(r') \times\left(\frac{1}{\omega-(\epsilon_j-\epsilon_i)+i\eta}-\frac{1}{\omega+(\epsilon_j-\epsilon_i)+i\eta}\right), \tag{3}$$

where the factor 2 is due to spin degeneracy, $f_i=\theta(\mu-\epsilon_i)$ is the Fermi distribution at $T=0$, and η is an infinitesimal. If $\bar{v}=f_{xc}=0$, then $\bar{\chi}=\chi^0$ and the independent particle-random phase approximation (IP-RPA) is recovered. In this approximation the spectrum is simply a sum over independent vertical transitions from valence (v) to conduction (c) states (atomic units are adopted throughout the text, if not otherwise specified),

$$\varepsilon_2^{\text{IP-RPA}}(\omega) = \frac{8\pi^2}{\Omega_0\omega^2}\sum_{vc}|\langle v|\hat{e}\cdot\mathbf{v}|c\rangle|^2\delta(\epsilon_c-\epsilon_v-\omega). \tag{4}$$

Here Ω_0 is the unit cell volume, $\hat{e}$ is the versor whose direction is along the polarization of the incident electromagnetic field and $\mathbf{v}=i[H,\mathbf{r}]$ is the velocity operator. If the Hamiltonian H contains only local potentials, then $\mathbf{v}=-i\nabla$. Otherwise, if, as in our case, nonlocal pseudopotentials are used, $\mathbf{v}=-i\nabla+i[V_{NL},\mathbf{r}]$. IP-RPA often yields poor descriptions of optical absorption, since local fields (LF) and excitonic effects, which are taken into account, respectively, by $\bar{v}$ and f_{xc}, may have a large influence on the spectra.

In finite systems what is experimentally measured is not ε_2, but the photoabsorption cross section σ [which is proportional to the dipole strength function $S, \sigma=(2\pi^2/c)S$]. However, σ is directly related to ε_2, which can still be calculated using expression (1) by setting the system in a periodic supercell of sufficiently large volume Ω_0, in order to make the interaction between periodic images negligible, and hence recover the physics of an isolated cluster,

$$\sigma(\omega) = \frac{\Omega_0}{c}\omega\varepsilon_2(\omega). \tag{5}$$

The use of a supercell is motivated by the fact that it allows one to use the same plane-wave basis and the same numerical machinery (e.g., fast Fourier transforms) as for infinite periodic crystals. In the limit of large Ω_0, the product $\Omega_0\cdot\varepsilon_2(\omega)$ becomes independent on Ω_0. Moreover, in this limit one finds $\bar{v}=v$, i.e., the contributions of $v_{G=0}$ becomes negligible. This means that, in practice, $\bar{\chi}_{G,G'}$ is the same as the usual reducible polarizability $\chi_{G,G'}$, defined by Eq. (2) with v (the standard Coulomb interaction) instead of $\bar{v}$. As a consequence, the imaginary part of ε_M (1) coincides (apart from the sign) with the imaginary part of the macroscopic *inverse* dielectric function,

$$\text{Im}\{\varepsilon_M^{-1}(\omega)\} = \lim_{\mathbf{q}\to 0}\text{Im}\{v_{G=0}(\mathbf{q})\chi_{G=G'=0}(\mathbf{q},\omega)\}. \tag{6}$$

Physically, this means that plasmon peaks [poles of $\varepsilon_M^{-1}(\omega)$] coincide with optical absorption peaks [poles of $\varepsilon_M(\omega)$], since both are related to the same collective charge density oscillation, once local field effects are taken into account.

For the photoabsorption cross section the following sum rule is valid:

$$\frac{c}{2\pi^2}\int_0^{+\infty}\sigma(\omega)d\omega = N \tag{7}$$

where N is the number of electrons of the system. If σ is calculated using nonlocal pseudopotentials, however, then (7) contains also correction terms involving matrix elements of the commutator and double commutator of the potential with the position operator.

The use of a large supercell to simulate a finite, isolated system makes the implementation of the effects due to f_{xc} in Eq. (2) more delicate than for the case of $\bar{v}$ alone, particularly in the case of the adiabatic local density approximation (ALDA). In this case, f_{xc} takes the form

$$f_{xc}^{\text{ALDA}}(r,r') = \delta(r-r')\frac{\partial V_{xc}^{\text{LDA}}(\rho(r),r)}{\partial\rho(r)}. \tag{8}$$

Since in a supercell there are large spatial regions where the charge vanishes, and $\partial V_{xc}^{\text{LDA}}/\partial\rho\to\infty$ for $\rho\to 0$, the term $T=\chi_0 f_{xc}^{\text{ALDA}}$ in (2) cannot be simply calculated as the product in reciprocal space between the Fourier transforms of χ_0 and f_{xc}^{ALDA},

$$T_{G_1,G_2}(\mathbf{q},\omega) = \sum_{G_3}\chi^0_{G_1,G_3}(\mathbf{q},\omega)f^{xc,\text{ALDA}}_{G_3-G_2} \tag{9}$$

because the Fourier transform of the divergent function f_{xc}^{ALDA} is ill defined. The "naive" way to overcome this difficulty, i.e., by introducing a cutoff for low densities, zeroing ρ and f_{xc}^{ALDA} in the empty space region, leads to arbitrary results, depending on the particular cutoff chosen. However, since the product $\chi_0 f_{xc}^{\text{ALDA}}$ is well behaved everywhere, $T_{G_1,G_2}(\mathbf{q},\omega)$ can be obtained by Fourier transforming this product, first calculated in real space,

$$T(r_1,r_2,\omega) = \sum_{n_1,n_2}\frac{f_{n1}-f_{n2}}{\omega-(\epsilon_{n2}-\epsilon_{n1})+i\eta}\tilde{\rho}_{n1n2}(r_1)\gamma_{n1n2}(r_2) \tag{10}$$

here $\tilde{\rho}_{n1n2}(r)=\varphi^*_{n1}(r)\varphi_{n2}(r)$ and $\gamma_{n1n2}(r)=\tilde{\rho}^*_{n1n2}(r)f_{xc}^{\text{ALDA}}(r)$. In addition, the $\mathbf{q}\to 0$ limit in $T_{G_1,G_2}(\mathbf{q},\omega)$ must be addressed with care, keeping into account the leading term in the integral of $\tilde{\rho}_{n1n2}(r)$ when n_1 and n_2 are, respectively, a valence and a conduction state. A detailed illustration can be found, e.g., in Appendix B of Ref. 15.

III. RESULTS

A. Equilibrium geometries and structural relaxation induced by oxygen

Our structural results for the two test systems (silane and silanone) compare very well with the experimental data (Refs. 16 and 17, respectively): the maximum discrepancy on the bond lengths—see Fig. 7 for silanone—does not exceed 1.3%. We are not aware of any experimental data on the structural parameters of $Si_{10}H_{16}$; however, available DFT calculations yield a Si-Si distance between 2.32 Å (LDA)

TABLE I. HOMO-LUMO gap (in eV), calculated within DFT-LDA for the two test systems (silane and silanone) and for the adamantanelike cluster $Si_{10}H_{16}$. Our results are compared with other theoretical results for the same systems (columns 3–7). Data from Refs. 11 and 12 have been estimated from graphical representations.

Cluster	This work	Ref. 23	Ref. 24	Ref. 11	Ref. 12	Ref. 25
SiH_4	7.85	7.8	7.85	7.7		7.9
H_2SiO	3.62			3.6		
$Si_{10}H_{16}$	4.59			4.6	4.6	4.6

(Ref. 18) and 2.35 Å (GGA) (Ref. 6), in good agreement with our result of 2.31 Å. Available DFT calculations can also be compared with our results for what concerns the HOMO-LUMO gaps, in all cases (i.e., SiH_4, H_2SiO, and $Si_{10}H_{16}$) the agreement is excellent (see Table I).

We now consider the structural modifications induced by oxidation of $Si_{10}H_{16}$. As expected, Si-H bond lengths are almost unaffected; however, also the Si-Si bonds are found to undergo very limited changes, as illustrated in Table II. Bond angles, on the contrary, register very large changes, up to 37% in $Si_{10}H_{14}O$-sym. The isomer with double Si=O bond (i.e., $Si_{10}H_{14}O$-double) undergoes smaller relaxations than isomers with bridge bonds: this observation is in agreement with the results of Luppi and Ossicini[12] for other nanocrystals. Moreover, in accordance with the works of Puzder *et al.*,[11] we find that $Si_{10}H_{14}O$-sym (the stablest isomer) has a larger binding energy (by 1.7 eV) than $Si_{10}H_{14}O$-double. The relative stability of the other bridge-bonded isomer ($Si_{10}H_{14}O$-asym) is very similar to that of the double-bonded cluster (i.e., +1.6 eV), while the interstitially-bonded isomer ($Si_{10}H_{14}O$-interst) is found at a significantly higher energy (+2.6 eV with respect to $Si_{10}H_{14}O$-sym). In $Si_{10}H_{14}O$-double the Si=O bond has a very similar length (1.529 Å) as the one obtained by Luppi and Ossicini in $Si_{14}H_{18}O$ (1.524 Å); the strain of Si-Si bond lengths and the angle variation due to oxidation are also essentially the same.

The structural modification induced by the creation of a Si-O-Si bridge over a covalent Si-Si bond can be compared with those taking place on Si surfaces exposed to oxygen. Considering, e.g., the case of Si(100), one finds a significant increase of the Si-Si distance only when the oxidized Si-Si bond is between two undercoordinated atoms, like in Si dimers of the (2×1), $p(2\times2)$ or $c(4\times2)$ reconstructions. When, on the contrary, oxygen adsorbs over a "bulklike" Si-Si bond (like that of backbonds in the same surfaces), the Si-Si distance increases much less, despite the significant changes in valence charge distribution.[19]

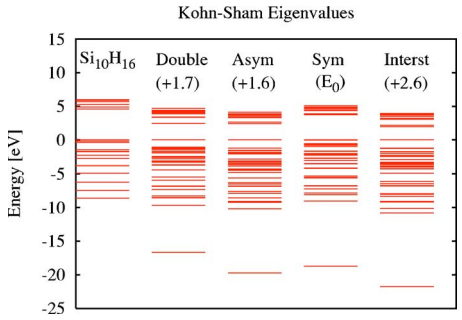

FIG. 2. (Color online) Effect of the oxidation on the $Si_{10}H_{16}$ Kohn-Sham eigenvalues. The four inequivalent isomers of $Si_{10}H_{14}O$ give rise to substantially different electronic structures. HOMO levels have been aligned. Binding energies (in eV) for each isomer are reported and compared with the binding energy E_0 of the stablest isomer, which is $Si_{10}H_{14}O$-sym (see text).

Besides structural modifications, oxidation induces significant changes in the electronic properties. First, one expects a splitting of the degenerate KS levels of $Si_{10}H_{16}$, due to the symmetry reduction; second, adding an oxygen atom will introduce electronic states with respect to the nonoxidized cluster. As shown in Fig. 2, an isolated strongly bound level appears, related to the 2*s* orbital of oxygen. Furthermore, there are oxygen-related states appearing inside the energy region of the HOMO-LUMO gap of $Si_{10}H_{16}$. As it has been already described in previous works,[11,12,20] oxidation of the considered system induces hence a *reduction* of the HOMO-LUMO gap.[29] Our results for the different systems studied are summarized in Table III. An important remark which comes out from the analysis of our results is that the intensity of the gap reduction depends more strongly on the specific isomer considered than on the type of bond. In agreement with Puzder *et al.*[11] and Luppi and Ossicini,[12] we find that the formation of a double bond determines a strong reduction of the gap; in comparison, the gap reduction in $Si_{10}H_{14}O$-sym is quite small. However, in the remaining two isomers with bridge bond (not considered in Ref. 11) the calculated gap turns out to be even smaller than in $Si_{10}H_{14}O$-double.

Simulating the oxidation of $Si_{12}H_{16}$ and $Si_{14}H_{20}$, Luppi and Ossicini[12] also studied a different kind of bridge bond with respect to those in Ref. 11, but similar to the one that in our case leads to $Si_{10}H_{16}O$. In agreement with their conclusions, we find that this other oxidation mechanism is much less effective in the reduction (only 0.59 eV) of the HOMO-LUMO gap of the clean nanocrystal.

TABLE II. Oxidation-induced structural relaxation in $Si_{10}H_{14}O$. The variations (in % of the values for $Si_{10}H_{16}$) are reported for the mean, maximum, and minimum values of the interatomic bond lengths, for the four isomers considered.

	$Si_{10}H_{14}O$-double			$Si_{10}H_{14}O$-asym			$Si_{10}H_{14}O$-sym			$Si_{10}H_{14}O$-interst		
Bond	Mean	Max	Min	Mean	Max	Min	Mean	Max	Min	Mean	Max	Min
Si-Si	+0.1	+0.4	−0.1	−0.5	+1.5	−4.6	+0.3	+1.1	−0.6	+1.6	+6.2	+0.0
Si-H (1)	−0.1	+0.0	−0.2	+0.2	+0.4	+0.1	+0.0	+0.0	+0.0	+0.3	+0.3	+0.3
Si-H (2)	−0.1	−0.1	−0.1	+0.0	+0.2	−0.3	−0.1	+0.0	−0.1	−0.2	+0.1	−1.2

TABLE III. HOMO-LUMO gap (in eV), calculated within DFT-LDA for all the oxidized nanocrystals considered. In columns 3–5, the difference Δ with respect to the "clean" $Si_{10}H_{16}$ nanocrystal is reported. Data from Refs. 11 and 12 have been estimated from graphical representations.

Cluster	HOMO-LUMO gap This work	Δ This work	Δ Ref. 11	Δ Ref. 12
$Si_{10}H_{14}O$-double	2.47	−2.12	−2.1	−2.1
$Si_{10}H_{14}O$-asym	2.42	−2.17		
$Si_{10}H_{14}O$-sym	3.74	−0.85		−0.9
$Si_{10}H_{14}O$-interst	1.95	−2.64		
$Si_{10}H_{16}O$	4.00	−0.59		

B. Optical spectra

In order to be able to compare quantitatively our results with other calculations, which sometimes[6,12] do not keep into account the effects of the commutator $[V_{NL},\mathbf{r}]$ between the nonlocal pseudopotentials and the position operator in matrix elements of (4), we first have to assess the importance of these effects. The additional term has no effect on the positions of the peaks in the spectrum, but it affects oscillator strengths. Therefore, it is important to take it into account if one is interested in the f-sum rule integral of Eq. (7). We show in Fig. 3 the effects of the inclusion of the commutator in the case of $Si_{10}H_{16}$. The additional term is found to reduce the absorption intensity, yielding a correction of 14% in the integral of Eq. (7). In the other clusters considered here, the effect is similar. In all cases, one has a comparable—and limited—reduction of the absorption intensity,[21,30] but no dramatic changes in the spectral line shape (the relative heights of the peaks are preserved).

A much more drastic effect is the one of local fields, which were also not always included in previous calculations (see, e.g., Ref. 12). LF effects, and the numerical methods allowing one to keep them into account, are common to two different classes of calculations, those based on many-body perturbation theory (e.g., the GW plus Bethe-Salpeter approach[14,22]) and calculations based on TDDFT, as those

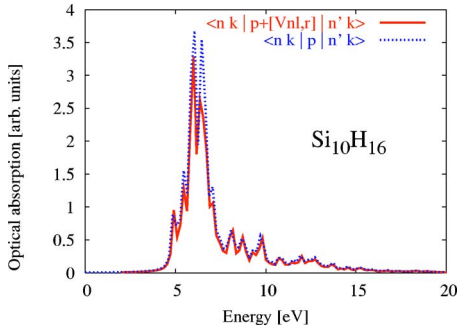

FIG. 3. (Color online) Effect of the inclusion of the commutator between the nonlocal pseudopotential and the position operator in Eq. (4), exemplified in the case of $Si_{10}H_{16}$ at the IP-RPA level (see text).

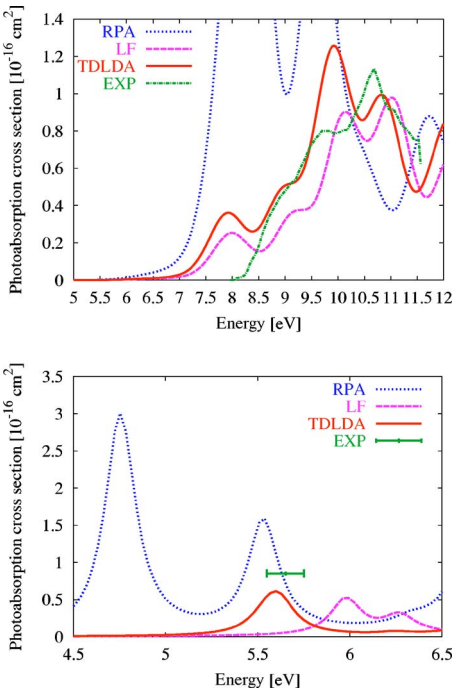

FIG. 4. (Color online) Calculated absorption spectrum for silane (upper panel) and silanone (bottom panel), at the three levels of approximation considered, IP-RPA (dotted line); including local fields (dashed line); and including also exchange-correlation effects at the ALDA level (full line). For silane all the theoretical spectra have been broadened with a width of about 0.3 eV. The experimental data from Ref. 26 are also reported for comparison (dotted-dashed line). For silanone a line broadening of about 0.2 eV has been used and the spectrum has been averaged over the three polarization directions. The horizontal bar represents the experimental edge of optical absorption, reported at 5.65±0.1 eV in Ref. 27.

presented in this work. Numerically, we include LF effects through Eq. (2), which is solved for $\bar{\chi}_{G=G'}$, by keeping into account the contribution of $\bar{v}$ and neglecting f_{xc}. When also the excitonic effects contained in f_{xc} are considered, e.g., within the adiabatic local density approximation [Eq. (8)], the spectra do not undergo great changes with respect to the results previously obtained neglecting f_{xc}. In fact a common behavior found in all systems studied is that local field effects give the largest contribution to the modification of the spectra from the starting IP-RPA ones to the final TDLDA results. This can be traced back to the strong inhomogeneity of finite systems, in clear contrast to what happens in bulk silicon, where LF effects are found to give very small contributions.[22] However, an important difference emerges comparing the behavior of SiH_4 and $Si_{10}H_{16}$ spectra with those of H_2SiO. In the first two clusters, as Benedict *et al.*[25] have observed, the absorption onset in TDLDA has practically the same position as in the IP-RPA calculation, despite the strong reduction of the peak strength (see, e.g., upper panel of Fig. 4). In silanone, instead, the inclusion of LF effects and f_{xc} is actually effective in shifting the position of the first peak, hence moving the absorption onset and edge (see bottom panel of Fig. 4). In other systems considered, e.g., $Si_{10}H_{14}O$-asym and $Si_{10}H_{16}O$, the situation is interme-

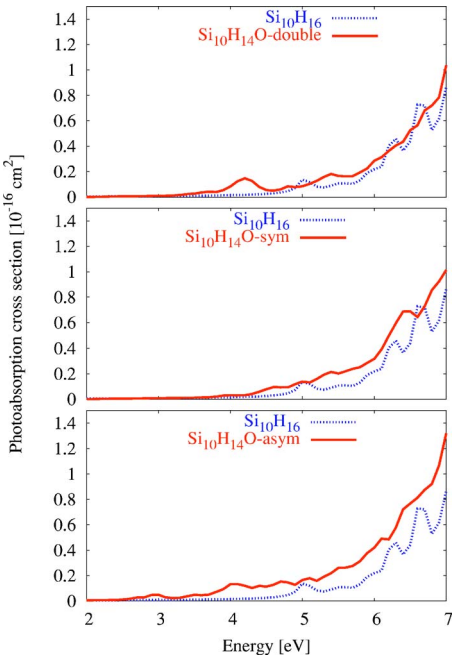

FIG. 5. (Color online) Absorption spectra, calculated at the full TDLDA level, for three isomers of $Si_{10}H_{14}O$ (see Fig. 1), compared with the spectrum of the "clean" $Si_{10}H_{16}$ nanocrystal. From top to bottom, $Si_{10}H_{14}O$-double, $Si_{10}H_{14}O$-sym, and $Si_{10}H_{14}O$-asym. A Lorentzian line broadening of 0.1 eV has been used, and the spectra have been averaged over the three polarization directions.

diate, effects beyond IP-RPA affect the first peak position with a shift of about 0.3 eV.

In Fig. 4 the theoretical spectra for silane and silanone are also compared with the experimental data of Refs. 26 and 27, respectively. In the case of SiH_4, the spectral shape shows an overall agreement, especially for the relative intensities of the three main peaks. However, the calculated absorption edge is underestimated with respect to the experiment, a well-known result common to previous studies (see, e.g., Refs. 25 and 28), no matter if the f_{xc} contributions to Eq. (2) are kept into account or not. The situation is better in the case of silanone, where the experimental absorption edge has been measured at 5.65 ± 0.1 eV (we are not aware of any available experimental data for the whole absorption spectrum). The calculated spectrum including LF effects *and* f_{xc} does agree with the measured value, while the absorption edge would be underestimated by almost 1 eV in IP-RPA, and overestimated by more than 0.5 eV in the LF-only calculation. Unfortunately, for larger clusters precise experimental data on the absorption spectra are still lacking. Comparing our results for the adamantanelike $Si_{10}H_{16}$ with those of previous calculations, namely those of Ref. 25, we find an excellent agreement.

C. Effects of oxidation on the optical gap

As shown in Fig. 5, oxidation of $Si_{10}H_{16}$ is always accompanied by a redistribution of oscillator strength towards the low-energy regions, where structures may also be created. We focus now on the effects that oxidation induces on the *optical gap*. Our results for the redshifts of the optical gap are summarized in Table IV. In all cases except $Si_{10}H_{14}O$-double, the second column (IP-RPA) coincides with the third column in Table III, since the optical gap coincides with the HOMO-LUMO gap. In $Si_{10}H_{14}O$-double the HOMO-LUMO transition is dipole forbidden, so the IP-RPA optical gap corresponds to the HOMO-(LUMO+1) transition. The most important remark is that the effects of oxidation on the optical gap are quite strongly isomer dependent, even limiting the comparison to the most similar systems, like $Si_{10}H_{14}O$-sym and $Si_{10}H_{14}O$-asym. Another relevant point is that the inclusion of local fields visibly affects the size of the redshift due to oxidation, generally reducing it (except for the case of $Si_{10}H_{14}O$-double), but does not change qualitatively its behavior. As for the inclusion of the exchange-correlation term, f_{xc}, it turns out to have almost no influence on the size of the redshift, since absorption edges of "clean" and oxidized clusters are shifted by the same amount by f_{xc}.

TABLE IV. Redshift (in eV) of the calculated *optical* gap, after oxidation of $Si_{10}H_{16}$. Four isomers of $Si_{10}H_{14}O$, and $Si_{10}H_{16}O$, are listed at the three increasing levels of approximation considered, IP-RPA, local fields only, and TDLDA (see text).

System	IPRPA	LF	TDLDA
$Si_{10}H_{14}O$-double	1.23	1.3	1.3
$Si_{10}H_{14}O$-asym	2.17	2.0	2.0
$Si_{10}H_{14}O$-sym	0.85	0.8	0.8
$Si_{10}H_{14}O$-interst	2.64	2.55	2.5
$Si_{10}H_{16}O$	0.59	0.4	0.4

The above conclusions are important since most of the previous calculations of the redshift induced by oxidation were performed at the bare IP-RPA level (see, e.g., Ref. 12). The fact that the inclusion of LF and f_{xc} effects does not change qualitatively the redshifts calculated in IP-RPA, despite the large effects that LF have on the spectra themselves, is reassuring, and confirms that calculations of *relative changes* in the optical gap of Si nanostructures can be quite safely evaluated at the IP-RPA level, even if the *absolute* value of those gaps could be quite strongly underestimated.

Coming back to to the strong isomer dependence of the redshift induced by oxidation, we notice that it is not possible to explain this dependence as simply based on the type of bond (bridge or double). For example, it is true that $Si_{10}H_{14}O$-double undergoes a larger redshift than $Si_{10}H_{14}O$-sym, but another bridge-bonded cluster, $Si_{10}H_{14}O$-asym, undergoes an even larger redshift. A more systematic explanation emerges from the analysis of the spatial localization of the Kohn-Sham orbitals near to the Fermi level, for all the systems considered. It turns out that the origin of the different behaviors among oxidized nanocrystals can be traced back to the different localization of the states involved in transitions which determine the optical gap, and in particular to the proximity of those states to the oxygen atom. As a matter of fact, both in $Si_{10}H_{14}O$-double and $Si_{10}H_{14}O$-asym such states are directly related to the oxygen atom (e.g., in $Si_{10}H_{14}O$-double HOMO and LUMO

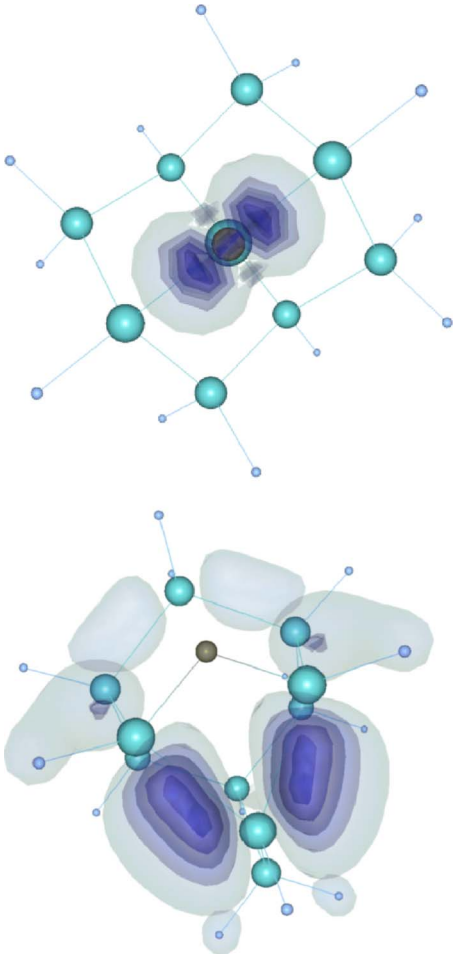

FIG. 6. (Color online) Spatial localization of the HOMO orbital, for $Si_{10}H_{14}O$-double (top) and $Si_{10}H_{14}O$-sym (bottom). In the former case the observed optical gap reduction after oxidation is substantially larger (see text).

are clearly *p* states of oxygen, as in silanone) and in these cases the gap reduction is large. A typical image of the HOMO orbital of $Si_{10}H_{14}O$-double is shown in the upper panel of Fig. 6. Instead, in $Si_{10}H_{14}O$-sym, which displays a small gap reduction, the HOMO orbital is completely localized on Si-Si bonds, and vanishes on the O atom, as shown in the lower panel of the same figure.

IV. CONCLUSIONS

In conclusion, our results on six small prototypical oxidized silicon clusters (H_2SiO, $Si_{10}H_{16}O$, and four different isomers of $Si_{10}H_{14}O$) show that (i) insertion of an O atom in both bond-bridge positions, or forming a double Si═O bond, induces a redshift of the optical absorption edge, more pronounced in the case of double Si═O bonds (in agreement with previous calculations); (ii) the amount of this redshift is strongly isomer dependent, being directly related to the localization of the HOMO orbital of the nanocrystal after oxidation, more than to the specific type of bridge bond; (iii) local field effects play an important role, and generally reduce the amount of the redshift induced by oxidation, with respect to the results obtained in IP-RPA; (iv) the effects of pseudopotential nonlocality are limited to a small reduction of the absorption intensity and are only evident on the *f*-sum rule integrals.

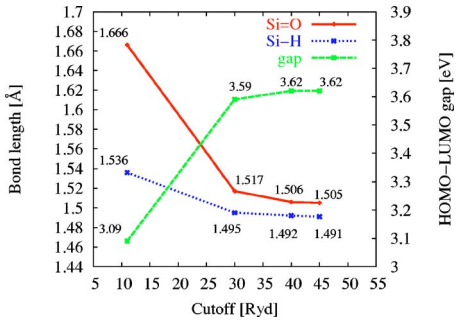

FIG. 7. (Color online) Convergence of the interatomic Si-O and Si-H bond lengths (full and dotted lines, respectively) and the HOMO-LUMO gap (dashed line), as a function of the energy cutoff, shown in the case of silanone. The experimental values (Ref. 17) for Si-H and Si═O bond lengths in silanone are, respectively, 1.472 Å and 1.515 Å. [Similarly, for silane the experimental bond length (Ref. 16) is 1.4798 Å, and our result is 1.486 Å.]

ACKNOWLEDGMENTS

The authors acknowledge useful discussions with A. Incze, E. Degoli, S. Ossicini, and R. Del Sole, and we thank Katalin Gaál-Nagy for a critical reading of the paper. This work was funded in part by the EU's 6th Framework Programme through the NANOQUANTA Network of Excellence (NMP4-CT-2004-500198). Computer facilities at CINECA granted by INFM (Project ID No. 239488704824) are gratefully acknowledged.

APPENDIX: COMPUTATIONAL DETAILS AND NUMERICAL CONVERGENCE

Since our first step consists in obtaining LDA Kohn-Sham eigenfunctions and eigenvalues to be used as an input in subsequent calculations of optical spectra, we started with an accurate and well-converged calculation of the ground state geometry and electronic structure, for all the nanocrystals considered.

We employed the Car-Parrinello method,[13] with norm-conserving pseudopotentials and a plane wave (PW) basis in a supercell approach. All the structures have been relaxed until all the interatomic forces were less than 5×10^{-3} eV/Å. We carefully studied the convergence of the structural results with the volume of the supercell, and with the energy cutoff of the PW expansion. For $Si_{10}H_{16}$ we find a variation of less than 3×10^{-4} Ha in total energies, and less than 1×10^{-4} Bohr in bond lengths, comparing calculations made by doubling the volume of the supercells (16 000 and 31 250 $Bohr^3$). As shown in Fig. 7, Si-H and Si-O bond lengths are well converged, within less than 1%, using a kinetic energy cutoff of 30 Ryd. The same cutoff is sufficient to obtain an HOMO-LUMO gap for H_2SiO converged within 1%.

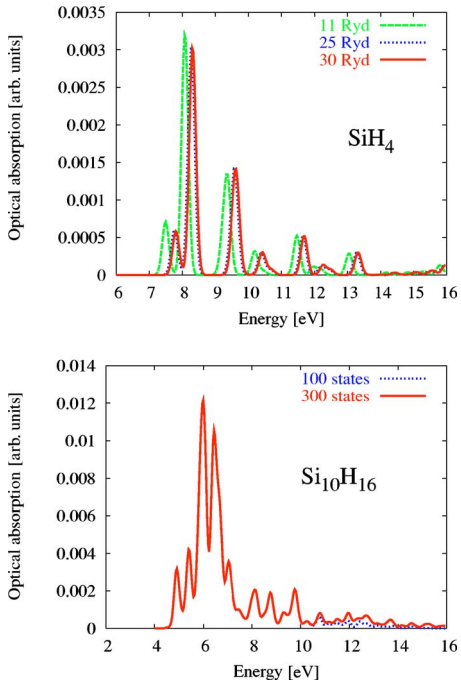

FIG. 8. (Color online) Convergence of the calculated absorption spectra at the IP-RPA level. Top, effect of the energy cutoff, exemplified for silane (full line, 30 Ryd; dotted line, 25 Ryd; dashed line, 11 Ryd); bottom, effect of the number of empty states included in Eq. (4), exemplified in the case of $Si_{10}H_{16}$ (full line, 300 states; dotted, 100 states). In the spectrum calculated with 100 states the energy difference between the HOMO and the highest state considered is 10.4 eV. It is 18.4 eV when 300 states are included. An artificial line broadening of 0.1 eV has been used.

Concerning the optical spectra, our zeroth-order approximation is IP-RPA. Hence we first checked the convergence of the IP-RPA spectra with respect to the energy cutoff, and to the total number of empty bands included in the calculations. In silane, the spectra obtained with cutoffs of 25 Ryd and 30 Ryd, shown in the top of Fig. 8, are already practically indistinguishable. The bottom panel of the same figure exemplifies the degree of convergence of the $Si_{10}H_{16}$ spectrum with respect to the number of empty bands.

The level of numerical convergence, established at the independent quasiparticle level, has been verified again at every following step. In order to study the convergence of local field corrections with the number of plane waves, i.e., with the size of matrices which are inverted in the solution of Eq. (2), we have first considered a simplified "single peak" model system, retaining only the first dipole allowed transition in the calculation of the optical spectrum of H_2SiO and $Si_{10}H_{16}$. These two model systems have the first allowed transition at quite similar energies ω_0 (4.75 eV and 4.59 eV, respectively), but the peaks undergo quite different shifts due to local fields. The absorption peak is in fact blueshifted by

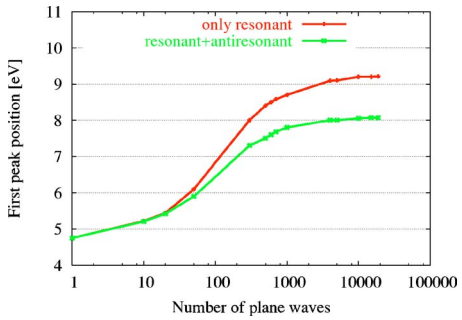

FIG. 9. (Color online) Convergence of the spectral shift induced by the inclusion of local field effects. Two model systems with a single valence-conduction transition have been investigated (see text), in order to analyze the effects of the coupling between the resonant and antiresonant terms in χ_0 [see Eq. (3)]. The results for silanone are reported, showing that the peak position calculated with the resonant term only (red — dark gray line) is overestimated by more than 1 eV with respect to the "exact" result (green — light gray line).

as much as 4.46 eV in the case of H_2SiO, and by only 0.455 eV in $Si_{10}H_{16}$ (this is a confirmation that the more the system is localized, the more important local fields are). Both resulting single-peak spectra are found to be fully converged with the use of about one-third of the total number of plane waves (see Fig. 9), corresponding to a kinetic energy cutoff of about 13 Rydbergs.[31]

The single-peak models also allow us to study easily, and check analytically, the effects of the coupling between the resonant and the antiresonant terms in the polarizability χ_0 [see Eq. (3)]. Neglecting the coupling, local fields induce only a rigid blueshift of the position of the peak in $\varepsilon_2(\omega)$, without affecting the peak amplitude.[32] Including the coupling has two effects: first, a reduction—proportional to the blueshift—of the intensity of the $\varepsilon_2(\omega)$ peak, in order to preserve the value of the integral (7); second, a modification of the shift with respect to the "resonant-only" calculation. However, naming K the absolute value of the shift due to the resonant term alone, one can easily demonstrate that if $K \ll \omega_0$, then the correction to the peak position due to the coupling is negligible. This is quite the case for the $Si_{10}H_{16}$ (K=0.455 eV), where the correction to the peak position due to the coupling is only 0.025 eV, while in H_2SiO, having K=4.46 eV and ω_0=4.75 eV, the coupling has a dramatic effect: the difference in the peak position between results obtained with and without the coupling is larger than 1 eV (Fig. 9). We checked that these conclusions remain valid also beyond the "single peak" model, i.e., when the spectrum is calculated by including *all* possible transitions, in this case K is substantially reduced (e.g., K=1.8 eV for H_2SiO), due to the interactions among different transitions, but the effect of the coupling on the energy of the first peak remains as large as 0.28 eV.

[1] L. T. Canham, Appl. Phys. Lett. **57**, 1046 (1990).
[2] L. Pavesi, L. Dal Negro, C. Mazzoleni, G. Franzò, and F. Priolo, Nature (London) **408**, 440 (2000).
[3] See, e.g., A. J. Williamson, J. C. Grossman, R. Q. Hood, A. Puzder, and G. Galli, Phys. Rev. Lett. **89**, 196803 (2002); C. S. Garoufalis, A. D. Zdetsis, and S. Grimme, *ibid.* **87**, 276402 (2001); S. Öğüt, J. R. Chelikowsky, and S. G. Louie, *ibid.* **79**, 1770 (1997); **80**, 3162 (1998); **83**, 1270 (1999) and references therein; J. P. Proot, C. Delerue, and M. Lannoo, Appl. Phys. Lett. **61**, 1948 (1992); G. Allan, C. Delerue, and M. Lannoo, Phys. Rev. Lett. **76**, 2961 (1996); M. Rohlfing and S. G. Louie, *ibid.* **80**, 3320 (1998); I. Vasiliev, S. Öğüt, and J. R. Chelikowsky, *ibid.* **86**, 1813 (2001); I. Vasiliev, Phys. Status Solidi B **239**, 19 (2003).
[4] See, e.g., S. Furukawa and T. Miyasato, Phys. Rev. B **38**, 5726 (1988); Y. Kanemitsu, H. Uto, Y. Masumoto, T. Matsumoto, T. Futagi, and H. Mimura, *ibid.* **48**, 2827 (1993); S. Schuppler *et al.*, *ibid.* **52**, 4910 (1995); T. van Buuren, L. N. Dinh, L. L. Chase, W. J. Siekhaus, and L. J. Terminello, Phys. Rev. Lett. **80**, 3803 (1998); J. von Behren, T. van Buuren, M. Zacharias, E. H. Chimowitz, and P. M. Fauchet, Solid State Commun. **105**, 317 (1998); J. P. Wilcoxon, G. A. Samara, and P. N. Provencio, Phys. Rev. B **60**, 2704 (1999); J. Valenta, R. Juhasz, and J. Linnros, Appl. Phys. Lett. **80**, 1070 (2002).
[5] A. Franceschetti and S. T. Pantelides, Phys. Rev. B **68**, 033313 (2003); A. Puzder, A. J. Williamson, J. C. Grossman, and G. Galli, J. Am. Chem. Soc. **125**, 2786 (2003); H-Ch. Weissker, J. Furthmüller, and F. Bechstedt, Phys. Rev. B **69**, 115310 (2004).
[6] E. Degoli, G. Cantele, E. Luppi, R. Magri, D. Ninno, O. Bisi, and S. Ossicini, Phys. Rev. B **69**, 155411 (2004).
[7] A. Puzder, A. J. Williamson, F. A. Reboredo, and G. Galli, Phys. Rev. Lett. **91**, 157405 (2003); I. Vasiliev and R. M. Martin, Phys. Status Solidi B **233**, 5 (2002); L. Mitas, J. Therrien, R. Twesten, G. Belomoin, and M. H. Nayfeh, Appl. Phys. Lett. **78**, 1918 (2001).
[8] See, e.g., Y. M. Niquet, C. Delerue, G. Allan, and M. Lannoo, Phys. Rev. B **62**, 5109 (2000).
[9] M. Palummo, G. Onida, R. Del Sole, and B. S. Mendoza, Phys. Rev. B **60**, 2522 (1999).
[10] M. V. Wolkin, J. Jorne, P. M. Fauchet, G. Allan, and C. Delerue, Phys. Rev. Lett. **82**, 197 (1999).
[11] A. Puzder, A. J. Williamson, J. C. Grossman, and G. Galli, Phys. Rev. Lett. **88**, 097401 (2002); J. Chem. Phys. **117**, 6721 (2002).
[12] M. Luppi and S. Ossicini, J. Appl. Phys. **94**, 2130 (2003); Phys. Status Solidi A **197**, 251 (2003); Mater. Sci. Eng., B **101**, 34 (2003).
[13] R. Car and M. Parrinello, Phys. Rev. Lett. **55**, 2471 (1985).
[14] G. Onida, L. Reining, and A. Rubio, Rev. Mod. Phys. **74**, 601 (2002).
[15] V. Olevano, M. Palummo, G. Onida, and R. Del Sole, Phys. Rev. B **60**, 14224 (1999).
[16] *CRC Handbook of Chemistry and Physics*, 79th ed., edited by D. R. Lide (CRC Press, Boca Raton, FL, 1998).
[17] M. Bogey, B. Delocroix, A. Walters, and J. Guillemin, J. Mol. Spectrosc. **175**, 421 (1996).
[18] G. Onida and W. Andreoni, Chem. Phys. Lett. **243**, 183 (1995).
[19] A. Incze, R. Del Sole, and G. Onida, Phys. Rev. B **71**, 035350 (2005).
[20] See, e.g., I. Vasiliev, J. R. Chelikowsky, and R. M. Martin, Phys. Rev. B **65**, 121302(R) (2002); A. B. Filonov, S. Ossicini, F. Bassani, and F. Arnaud d'Avitaya, *ibid.* **65**, 195317 (2002); A. B. Filonov, A. N. Kholod, V. E. Borisenko, A. L. Pushkarchuk, V. M. Zelenkovskii, F. Bassani, and F. A. d'Avitaya, *ibid.* **57**, 1394 (1998).
[21] O. Pulci, G. Onida, A. I. Shkrebtii, R. Del Sole, and B. Adolph, Phys. Rev. B **55**, 6685 (1997).
[22] S. Albrecht, L. Reining, R. Del Sole, and G. Onida, Phys. Rev. Lett. **80**, 4510 (1998).
[23] J. C. Grossman, M. Rohlfing, L. Mitas, S. G. Louie, and M. L. Cohen, Phys. Rev. Lett. **86**, 472 (2001).
[24] M. Rohlfing and S. G. Louie, Phys. Rev. B **62**, 4927 (2000).
[25] L. X. Benedict, A. Puzder, A. J. Williamson, J. C. Grossman, G. Galli, J. E. Klepeis, J. Y. Raty, and O. Pankratov, Phys. Rev. B **68**, 085310 (2003).
[26] U. Itoh, Y. Toyoshima, H. Onuki, W. Washida, and T. Ibuki, J. Chem. Phys. **85**, 4867 (1986).
[27] V. A. Radtsig, I. V. Berestetskaya, and S. N. Kostritsa, Kinet. Katal. **39**, 863 (1998), and references therein.
[28] M. A. L. Marques, A. Castro, and A. Rubio, J. Chem. Phys. **115**, 3006 (2001).
[29] In the case of the Si(100) surface, oxidation can even increase the energy gap (Ref. 19).
[30] In other systems, this term has been found instead to enhance the strengths (Ref. 21).
[31] The calculation for silanone yields 98.43% of the total shift using 27% of the total number of PWs, and 95.9% of the shift when only 15% of the PWs—corresponding to about 7 Ry—are used. In a similar way, the calculation for $Si_{10}H_{16}$ yields 96.7% of the shift with about 11% of the PWs.
[32] As a consequence, the *f*-sum rule cannot be fulfilled any more.